GADEST 20/24

Program and abstract booklet

20th meeting
Gettering and Defect Engineering
in Semiconductor Technology

Bad Schandau (Saxony, Germany)
September 8 - 13, 2024

Defect content characterization in solar cells with the assistance of machine learning

Oleg Olikh, and Oleksii Zavhorodnii

Taras Shevchenko National University of Kyiv, 64/13, Volodymyrska Street, 01601, Kyiv, Ukraine

Email: olegolikh@knu.ua

Integrating artificial intelligence into sustainable clean energy research, particularly using machine learning (ML) for defect characterization, is increasingly compelling. A prevalent strategy is to identify extended defects from electroluminescence images. Recently, however, there has been a notable shift in focus towards point defects [1,2]. Our research aims to create an efficient, low-cost machine learning-based methodology for evaluating recombination defects in solar cells (SCs) using current-voltage (IV) measurement data, eliminating the need for extra equipment.
To demonstrate our methodology, we focused on identifying iron-related defect concentrations in silicon SC. Fig. 1(a) presents the workflow. Using SCAPS-1D software, the performance of back surface field SCs under both standard AM1.5 and monochromatic (940 nm) illumination were modeled. Simulated IV curves captured the behaviour of iron- acceptor pairs and scenarios with only interstitial iron. Then the relative changes in short- circuit current εIsc, open-circuit voltage εVoc, efficiency $\varepsilon\eta$, and fill factor εFF were extracted. ML techniques – deep neural networks (DNN), random forest (RF), and gradient boosting (GB) – were employed to estimate iron concentrations. The accuracy of predictions from various models was compared using data obtained under different lighting conditions and with varying numbers (ranging from 4 to 7) of descriptors. In the simplest case, the descriptors included the SC's base depth and doping level, temperature, and εIsc. For cases involving 5, 6, and 7 descriptors, the $\varepsilon\eta$, εVoc, and εFF, were added respectively. The results are shown in Tables 1 and 2 and Fig. 1(b).

References:

[1] O. Olikh, O. Lozitsky and O. Zavhorodnii, *Prog Photovolt Res Appl.* **2022**, *30*, 648.
[2] Y. Buratti, J. Dick, Q.L. Gia and Z. Hameiri, *ACS Appl. Mater. Interfaces* **2022**, *14*, 48647.

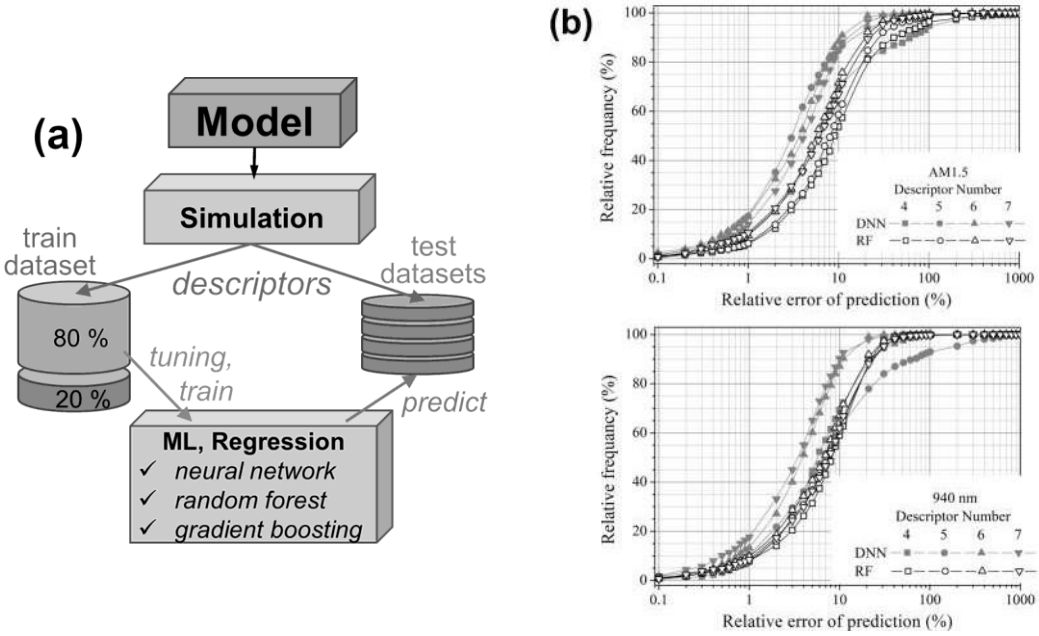

Fig. 1. (a) Workflow. (b) Fraction of samples for which the error does not exceed the threshold versus the threshold value for neural networks and random forest models. Top and down panels correspond to standard and monochromatic illumination, respectively.

Table 1. Results of 5-fold cross-validation for train dataset

Model	Illumination	Mean squared error (10^{-3})			
		Number of descriptors			
		4	5	6	7
DNN	AM1.5	42±5	9±3	4±2	2±1
	940 nm	10±5	6.1±0.4	6±2	1.5±0.7
RF	AM1.5	33±2	11±3	5±2	4±1
	940 nm	6±1	4.6±0.2	3.0±0.5	3.0±0.8
GB	AM1.5	34±2	9±2	5±2	4±1
	940 nm	4.2±0.6	3.5±0.2	2.3±0.6	2.1±0.5

Table 2. Prediction accuracy for test dataset

Model	Number of descriptors	Mean squared error (10^{-3})		Mean relative error (%)		R^2	
		Illumination					
		AM1.5	940 nm	AM1.5	940 nm	AM1.5	940 nm
DNN	4	58	6	53	10	0.905	0.977
	5	4	33	7	36	0.988	0.881
	6	0.9	0.6	5	5	0.992	0.993
	7	5	0.8	11	5	0.990	0.988
RF	4	41	3	142	11	0.930	0.968
	5	10	3	15	10	0.959	0.967
	6	4	3	10	9	0.972	0.956
	7	5	3	11	10	0.958	0.963
GB	4	33	3	43	8	0.947	0.965
	5	9	2	13	8	0.955	0.980
	6	5	2	10	7	0.969	0.967
	7	5	2	10	8	0.960	0.961